

## **LATERAL CAPILLARY FORCES AND TWO-DIMENSIONAL ARRAYS OF COLLOID PARTICLES AND PROTEIN MOLECULES**

N. D. Denkov, P. A. Kralchevsky and I. B. Ivanov  
Laboratory of Thermodynamics and Physico-chemical Hydrodynamics  
Faculty of Chemistry, Sofia University, 1126 Sofia, Bulgaria

### **ABSTRACT**

This paper presents a review of our recent studies on the lateral capillary forces and on their role in the formation of two-dimensional ordered arrays of colloidal particles or protein molecules. To reveal the mechanism of protein ordering in liquid films we carried out model experiments with micrometer sized latex particles. The films were formed on solid or liquid substrates. By variation of the electrolyte concentration, the particle charge and volume fraction we proved that neither the double layer repulsion, nor the van der Waals attraction between the particles, was responsible for the formation of the two-dimensional arrays. Direct microscope observations revealed that the process of ordering was triggered by attractive lateral capillary forces due to the overlap of the menisci formed around the particles. Two types of lateral capillary forces, flotation and immersion, could be distinguished and theory of these interactions was developed. The lateral capillary forces between a floating particle and a wall were also studied; they could be employed for precise determination of the shear surface viscosity.

### **INTRODUCTION**

The role of the lateral capillary forces in the formation of two-dimensional (2D) arrays of colloidal particles can be demonstrated by means of the following experiment [1]. A layer of thickness  $h$  formed from an aqueous suspension of latex particles (diameter 1.78  $\mu\text{m}$ ) is observed by microscope through the glass

substrate, Fig. 1a. When  $h$  is greater than the particle diameter one observes the Brownian motion of the particles, Fig. 2a. The layer thickness  $h$  is allowed to decrease due to water evaporation. Suddenly, at the moment when  $h$  becomes equal to the particle diameter, one observes a transition from disorder to order, Fig. 2b. This transition is triggered by the lateral capillary forces which are due to the overlap of the menisci formed around the particles [2-4], see Fig. 1b.

The interest in ordered two-dimensional (2D) colloid structures fixed on solid substrates [5-13] is stimulated by their possible applications in optical devices and some other techniques like data storage, microelectronics and synthetic membrane production [8-10, 12]. 2D arrays from micrometer and submicrometer latex particles, from a number of proteins and protein complexes [14-20] and even from viruses [16], were obtained. Since 3D crystals are obtained from a very limited number of integral membrane proteins, 2D crystallization provides a unique possibility for investigating their structure [15, 21]. The experience gained in the experiments on formation of ordered 2D structures from colloid particles and proteins shows that the choice of an appropriate substrate is of crucial importance for the ordering process.

The aim of the present study is to give a review of our recent studies of 2D array formation on solid and fluid substrates, as well as the recent theoretical and experimental advance in the field of the lateral capillary forces.

## STUDY OF THE MECHANISM OF 2D ARRAY FORMATION

### Solid Substrate

This is the case illustrated with the photographs in Fig. 2. To carry out the experiments we use the cell described in Ref. 1. A drop of the latex suspension of given volume and composition is placed upon a glass plate. The drop spreads over the accessible glass area encircled by a Teflon ring with an inner diameter of 14 mm. The system is mounted on the table of a metalographic microscope and is protected by a glass cover which allows illumination from above. The observations are performed through the bottom in reflected or transmitted light.

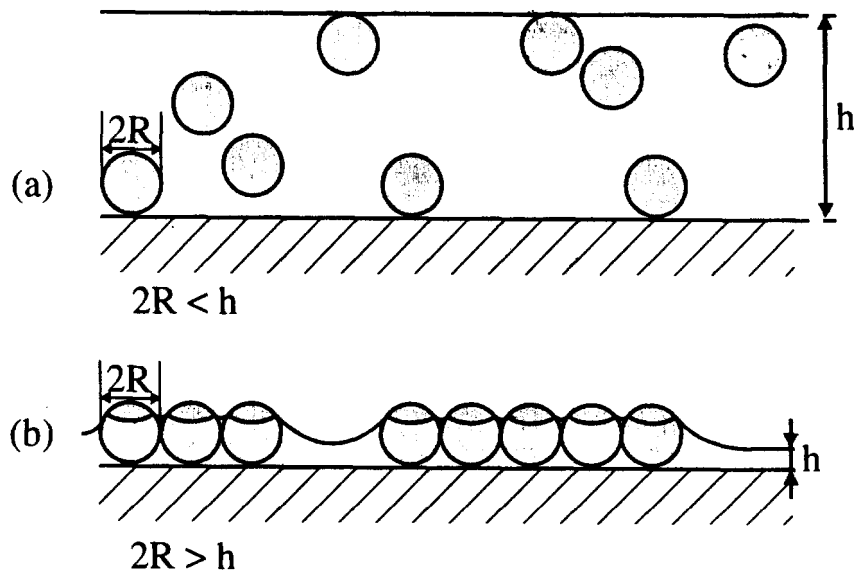


FIG. 1. Two-dimensional ordering of suspension particles in a liquid: (a) chaotic motion of the particles in a thick film; (b) capillary forces appear and cause aggregation after the particle tops protrude from the film.

In the experiments we observe the following. The slightly concave suspension layer gradually thins owing to the water evaporation; when its thickness in the center of the substrate becomes equal to the particle diameter, a nucleus of 2D crystal suddenly forms. The particles in the thicker layer encircling the nucleus begin to move towards the ordered zone, and upon reaching the boundary of the array, they are trapped in it (Fig. 2b). In some experiments we added 0.2 wt% glucose to the suspension and the flux of particles became slower.

The nature of the forces governing the ordering is revealed by the fact that in all experiments the 2D crystallization started when the thickness of the water layer became equal to the particle diameter [1, 22]. This implies that the 2D-crystal nuclei are formed under the capillary attraction arising when the tops of the particles protrude from the water layer (Fig. 1b). The respective attractive energy can be much larger than the thermal energy,  $kT$ , even with nanometer sized particles [4].

We were able to show that the subsequent stage of crystal growth is caused by a convective transport of particles towards the ordered nucleus. This effect also

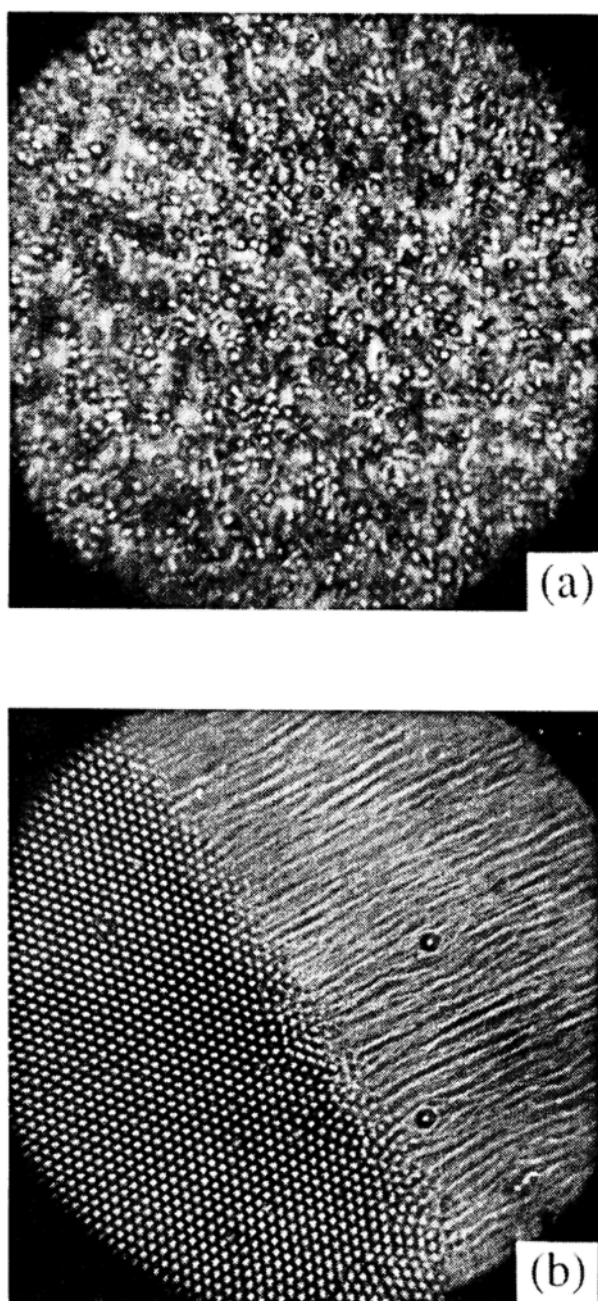


FIG. 2. (a) Photograph of latex particles (diameter  $1.78 \mu\text{m}$ ) involved in Brownian motion in a thick liquid film. (b) Photograph of the 2D array growth: the tracks of the particles rushing towards the ordered phase are seen.

appears when menisci form around the protruding tops of the hydrophilic particles in the nucleus (Fig. 1b). These menisci hinder the further thinning of the water layer in the nucleus. An intensive water influx from the thicker parts of the layer, which tends to compensate the water evaporation from the nucleus, appears next. This flux carries the suspended particles towards the nucleus. By decreasing or increasing the water evaporation rate we can speed up or slow down the convective particle transport. At increased humidity, we see a complete arrest of the process of ordering and even disintegration of the already ordered clusters.

### Fluid Substrate

We investigated also the possibility for application of perfluorinated oil (F-oil) as a liquid substrate for 2D array formation. We use F-oil because it possesses the appropriate features of the mercury substrate used in Refs. [17-20] (molecularly smooth and tangentially mobile surface) and some additional advantages: (i) it is chemically inert and hazardless; (ii) it allows the merging and rearranging of already ordered domains into larger ones, (iii) the 2D structure formed can be gently deposited onto another surface after evaporation of all F-oil, and (iv) it is difficult to contaminate the fluorocarbon surface (the common surfactants adsorb poorly at the fluorocarbon-water interface [23]). In particular, we use perfluoromethyldecalin, PFMD (commercial name Flutec PP-7, Rhone Poulenc, S.A.) as a substrate. PFMD has a higher density than water. It has high vapor pressure at room temperature and can be easily evaporated after the formation of a 2D array. Thus, the obtained array can be transferred onto a solid substrate for fixation and investigation, see Fig.3.

The performed experiments [24] demonstrated that F-oil substrates could be applied to the formation of 2D ordered structures from latex particles or ferritin molecules. Under appropriate conditions, large and well ordered 2D arrays from latex particles were obtained. The results confirm that the capillary forces and the convective particle flux are the main factors governing the 2D array formation process. The quality of the arrays can be improved by controlling the evaporation rate and the meniscus shape. Ordered 2D clusters from ferritin molecules were

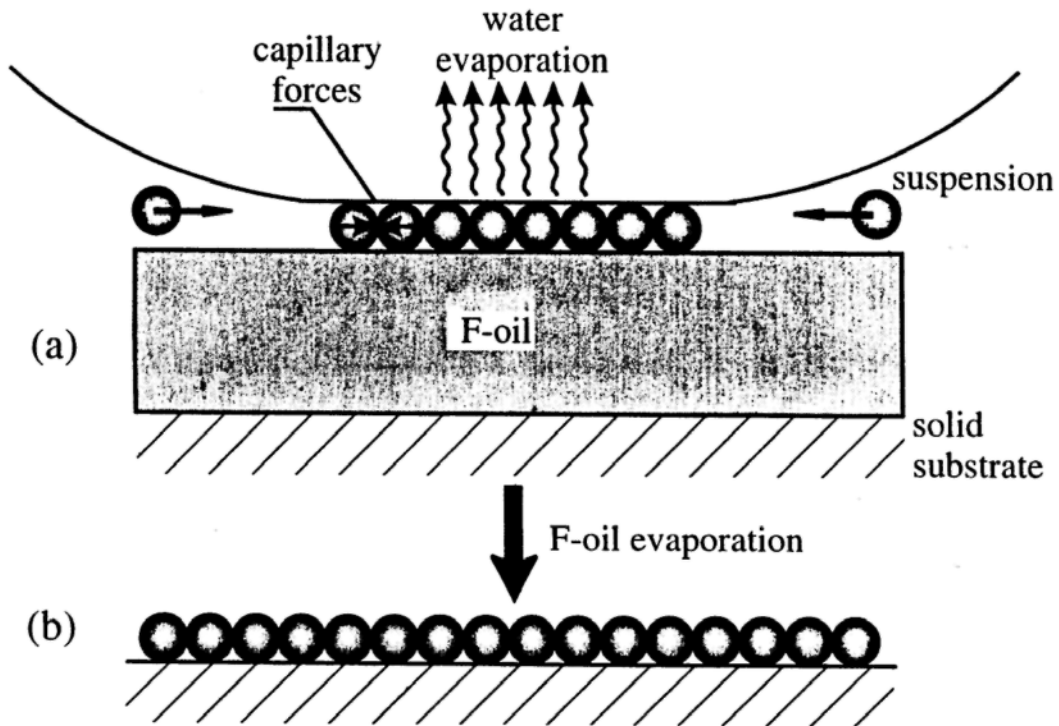


FIG. 3. Two-dimensional array formation on F-oil substrate: (a) 2D ordering of particles in an aqueous film over F-oil; (b) the formed 2D array is deposited on a solid substrate after evaporation of the water and the F-oil.

obtained in a similar way. They were then directly deposited onto the specimen grids and studied by TEM.

#### Freely Suspended Foam Film

We were able to show that well ordered arrays from nanometer sized particles could be produced even in freely suspended (foam) films without recourse to specific binding agents and supporting substrates. In this way ordered mono- and bilayers of latex spheres (144 and 66 nm in diameter) were obtained [25]. Remarkably, by this method we produced [25] ordered arrays of "soft" particles - monodisperse vesicles formed from the membrane protein bacteriorhodopsin and lipid [26]. For structural investigation of these samples we developed [25] a novel procedure for vitrification (ultra-rapid freezing [27]) of large in diameter foam

films, whose thickness was measured by direct video-microscope observation. The mean vesicle diameter, measured from digitized images obtained by transmission electron microscope at  $-196^{\circ}\text{C}$ , is 38.8 nm, while the mean center-to-center distance is 44.7 nm (see Figure 4). Features in the vesicle structure are discernible in the micrographs and a systematic structural analysis may lead to revealing the organization of the protein molecules within the vesicle.

## LATERAL CAPILLARY FORCES

### Flotation and Immersion Capillary Forces

The origin of the lateral capillary forces is the *deformation* of the liquid surface, which is supposed to be flat in the absence of particles. The larger the interfacial deformation created by the particles, the stronger the capillary interaction between them. The theoretical calculation of the capillary interaction force and energy is a difficult problem because the meniscus shape should be determined by solving the Laplace equation of capillarity which represents a nonlinear partial differential equation. In the pioneering work of Nicolson [28] the capillary interaction energy between two bubbles attached to a liquid surface was calculated by assuming that the surface deformation is a mere superposition of the deformations created by the single bubbles (so called "linear superposition approximation"). Several theoretical studies were published later concerning the interaction between spheres floating on a single interface [29] (where the superposition approximation was used) or between two infinite *horizontal* cylinders laying on an interface [29, 30]. In the latter case the general Laplace equation reduces to an ordinary differential equation.

In our works we extended further the theory by solving analytically the linearized Laplace equation (at small slopes of the meniscus around the particles) in bicylindrical coordinates [2-4, 31]. General expressions were obtained for the capillary interaction energy and force between two *vertical* cylinders and between two spheres [2, 3, 31], between a sphere and a vertical wall [32, 33], and other configurations [3, 31] without recourse to the superposition approximation

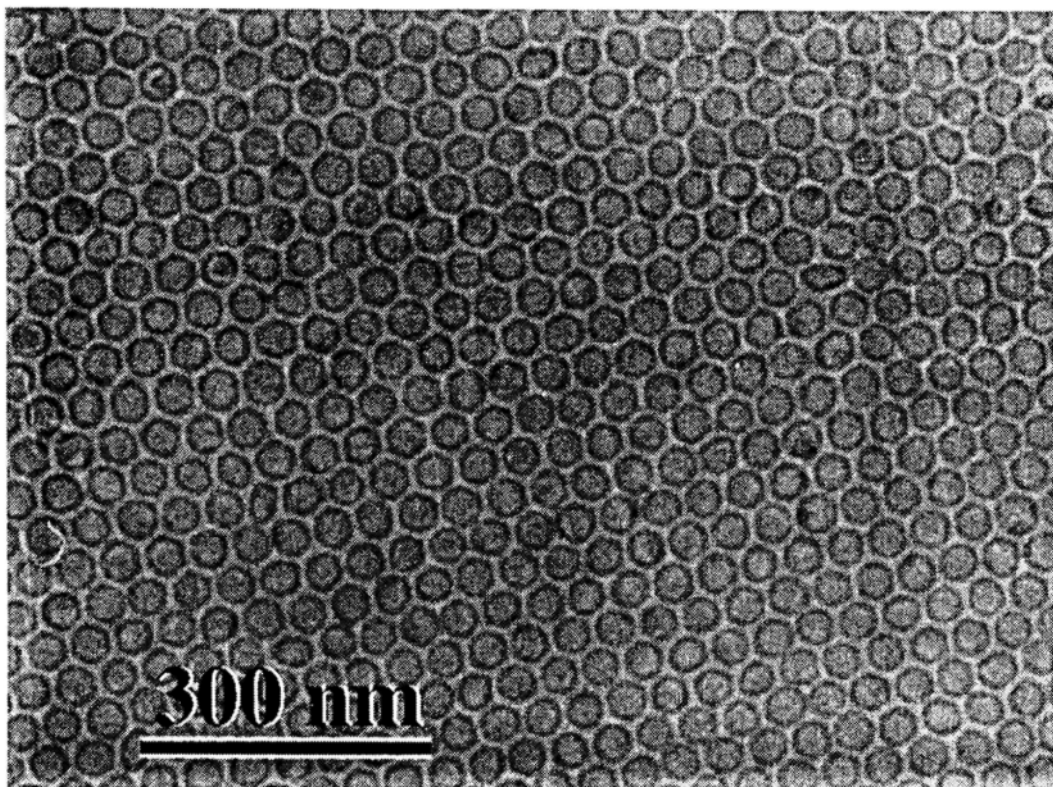


FIG. 4. Ordered monolayer of bacteriorhodopsin vesicles in vitrified aqueous film. The film thickness was 59 nm just before vitrification.

[28,29]. The comparison of the results stemming from the superposition approximation [28, 29] and from the more rigorous approach [31] showed that the superposition approximation could substantially underestimate the lateral capillary force at small interparticle separations - see Fig. 2 in Ref. [31].

It is known that two similar particles floating on a liquid interface attract each other [29, 31] - see Fig. 5a. This attraction appears because the liquid meniscus deforms in such a way that the gravitational potential energy of the two particles decreases when they approach each other. Hence the origin of this force is the *particle weight* (including the Archimedes force). We established that force of capillary attraction appears also when the particles (instead of being freely floating) are partially immersed in a liquid layer on a substrate [2-4] - see Fig. 5b. The deformation of the liquid surface in this case is related to the *wetting properties* of



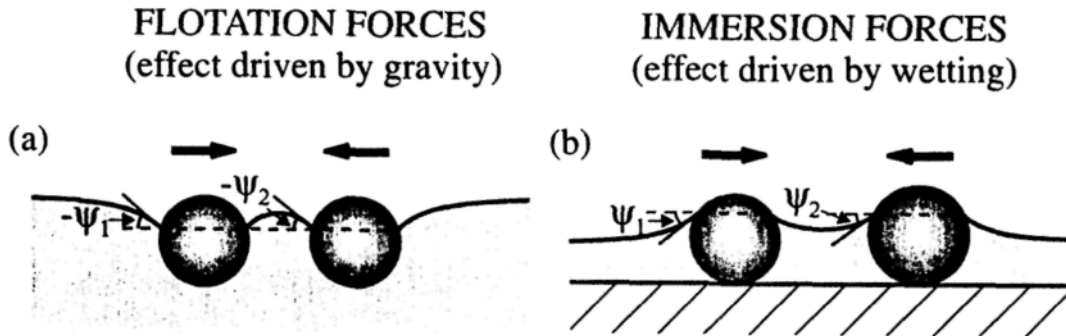


FIG. 5. Flotation and immersion lateral capillary forces due to the overlap of the menisci formed around particles attached to an interface.

the particle surface, i.e. to the position of the contact line and the magnitude of the contact angle, rather than to gravity.

To distinguish between the capillary forces in the case of floating particles, and in the case of partially immersed particles on a substrate, we called the former lateral *flotation* forces and the latter lateral *immersion* forces [4, 31]. These two kinds of force exhibit similar dependence on the interparticle separation but very different dependencies on the particle radius and the surface tension of the liquid. The flotation and immersion forces can be both attractive and repulsive. This is determined by the signs of the meniscus slope angles  $\psi_1$  and  $\psi_2$  at the two contact lines: the capillary force is attractive when  $\sin\psi_1\sin\psi_2 > 0$  and repulsive when  $\sin\psi_1\sin\psi_2 < 0$ . In the case of flotation forces  $\psi > 0$  for *light* particles (including bubbles) and  $\psi < 0$  for *heavy* particles. In the case of immersion forces between particles protruding from an aqueous layer  $\psi > 0$  for *hydrophilic particles* and  $\psi < 0$  for *hydrophobic particles*. When  $\psi = 0$  there is no meniscus deformation and, hence, there is no capillary interaction between the particles. This can happen with floating particles when the weight of the particles is too small to create significant surface deformation. The immersion force appears not only between particles in wetting films (Fig. 5b), but also in symmetric fluid films. The theory [3, 4, 29] provides the following asymptotic expression for calculating the lateral capillary force between two particles of radii  $R_1$  and  $R_2$  separated by a center-to-

center distance  $L$

$$F = 2\pi\sigma Q_1 Q_2 q K_1(qL) [1 + O(q^2 R_k^2)] \quad r_k \ll L \quad (1)$$

where  $\sigma$  is the liquid-fluid interfacial tension,  $Q_k = r_k \sin \psi_k$  ( $k = 1, 2$ ) is the "capillary charge" of the particle [4, 31], and  $r_1$  and  $r_2$  are the radii of the two contact lines; in addition

$$\begin{aligned} q^2 &= \Delta\rho g / \sigma && \text{(in thick films)} \\ q^2 &= (\Delta\rho g - \Pi') / \sigma && \text{(in thin films)} \end{aligned} \quad (2)$$

Here  $\Delta\rho$  is the difference between the mass densities of the two fluids,  $g$  is the gravity acceleration, and  $\Pi'$  is the derivative of the disjoining pressure with respect to the film thickness;  $K_1$  is the modified Bessel function. The asymptotic form of Eq. (1) for  $qL \ll 1$  ( $q^{-1} = 2.7$  mm for pure water),

$$F = 2\pi\sigma Q_1 Q_2 / L \quad r_k \ll L \ll q^{-1} \quad (3)$$

looks like a two-dimensional analogue of Coulomb's law, which explains the name "capillary charge" of  $Q_1$  or  $Q_2$ . Note that the immersion and flotation forces exhibit the same functional dependence on the interparticle distance, see Eqs. (1) and (3). On the other hand, their different physical origin results in different magnitudes of the "capillary charges" of these two kinds of capillary force. In the particular case when  $R_1 = R_2 = R$  and  $r_k \ll L \ll q^{-1}$ , one can derive [4, 31]

$$\begin{aligned} F &\propto (R^6 / \sigma) K_1(qL) && \text{for flotation force} \\ F &\propto \sigma R^2 K_1(qL) && \text{for immersion force.} \end{aligned} \quad (4)$$

Hence, the flotation force decreases, while the immersion force increases, when the interfacial tension  $\sigma$  increases. Besides, the flotation force decreases much more strongly with the decrease of  $R$  than the immersion force. Thus  $F_{\text{flotation}}$  is negligible for  $R < 10$   $\mu\text{m}$ , whereas  $F_{\text{immersion}}$  can be significant even when  $R = 10$  nm [12]. Hence, the immersion forces are among the main factors causing the observed self assembly of small colloidal particles (Fig. 2) and protein macromolecules [17, 18] confined in thin liquid films or lipid bilayers [4, 34].

In the case of interactions between integral proteins in lipid bilayers we took into account also the elasticity of the bilayer interior [34]. The calculated

energy of capillary interaction between membrane proteins turned out to be of the order of several  $kT$ ; hence, this interaction could have an important contribution to the observed aggregation of membrane proteins [34]. We extended the theory of the lateral capillary forces also to the case of particles captured in a *spherical* (rather than planar) thin liquid film or vesicle [35].

Lateral capillary forces between vertical cylinders or between spherical particles were measured by means of sensitive electromechanical balance [36], piezo-transducer balance [37] and torsion micro-balance [38, 39]. Good agreement between theory and experiment was established [37-39].

### Capillary Image Forces

The overlap of the meniscus around a floating particle with the meniscus on a vertical wall gives rise to a particle-wall interaction, which can be both repulsive and attractive. An example for a controlled meniscus on the wall is shown in Fig. 6, where the "wall" is a hydrophobic polytetrafluorethylene (PTFE) plate, whose position along the vertical can be precisely adjusted and varied.

We analyzed theoretically two types of boundary conditions at the wall: fixed contact *line* (Fig. 6) or, alternatively, fixed contact *angle*. In particular, the lateral capillary force exerted on the particle depicted in Fig. 6 is given by the following asymptotic expression [33]:

$$F = -\pi\sigma \left[ 2Q_2 q H e^{-qx} + q \left( r_2 q H e^{-qx} \right)^2 - 2q Q_2^2 K_1(2qx) \right] \quad (5)$$

Here  $Q_2$  and  $r_2$  are the particle capillary charge and contact line radius,  $H$  characterizes the position of the contact line on the wall with respect to the nondisturbed horizontal liquid surface (Fig. 6);  $x$  is the particle-wall distance;  $q$  is defined by Eq. (2) (thick films). The first term in the right-hand side of Eq. (5) expresses the gravity force pushing the particle to slide down over the inclined meniscus created by the wall; the second term originates from the pressure difference across the liquid meniscus on the wall; the third term expresses the so-called "capillary image force", that is the particle is repelled by its mirror image with respect to the wall surface [33].

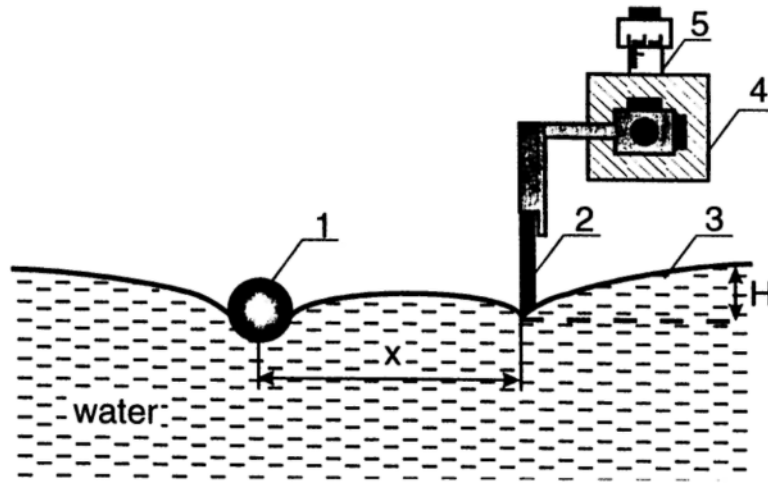


FIG. 6. Experimental set up for studying the particle-wall capillary interaction: (1) floating particle, (2) PTFE plate, (3) meniscus due to the presence of the wall, (4) micrometric table, and (5) precise micrometric screw for adjustment of the plate position.

We carried out static [40] and dynamic [41] measurements with particles near walls. In the static measurements the equilibrium distance of the particle from the wall (the distance at which  $F = 0$ ) was measured and a good agreement with the theory was established [40]. In the dynamic experiments [41] knowing the capillary force  $F$ , Eq. (5), and measuring the particle velocity,  $\dot{x}$ , one can determine the drag force,  $F_d$  exerted on the particle

$$F_d = m\ddot{x} - F, \quad F_d \equiv 6\pi\eta R_2 f_d \dot{x} \quad (6)$$

where  $R_2$ ,  $m$  and  $\ddot{x}$  are the particle radius, mass and acceleration,  $\eta$  is the viscosity of the liquid, and  $f_d$  is the dimensionless drag coefficient. If the particle were in the bulk liquid,  $f_d$  would be equal to 1 and  $F_d$  would be given by the known Stokes formula. In general,  $f_d$  differs from unity because the particle is attached to the interface. The experiment [41] gave  $f_d$  varying between 0.68 and 0.54 for particle contact angle varying from  $49^\circ$  to  $82^\circ$ ; the data were in a very good quantitative agreement with the hydrodynamic theory of the drag coefficient [42]. We found that when the floating particle was heavy enough to substantially deform the surrounding liquid surface, the measured values of  $f_d$  were several times larger than unity [41]. The later effect is due to the interfacial deformation, which travels with

the particle, thus increasing  $f_d$  [41]. The addition of surfactant strongly increased  $f_d$ . The latter effect was utilized to measure the surface viscosity of adsorption monolayers from low molecular weight surfactants [43], which was not accessible to the standard methods for measurement of surface viscosity.

## 2D ARRAYS OF PROTEINS AND VIRUSES

There are many arguments to claim that the lateral capillary forces, discussed above, may play a role in some of the procedures used for obtaining of 2D ordered arrays from protein molecules and viruses. For instance, Lewis and Engelman [44] demonstrated experimentally that the membrane protein bacteriorhodopsin forms 2D aggregates in lipid vesicles only when the mismatch between the hydrophobic belt of the protein and the bilayer hydrophobic thickness is greater than 0.4 nm. Similar observations were reported by Chen and Hubbell [45] for rhodopsin and by Huschilt et al. [46] for synthetic polypeptide. These results support the idea of Israelachvili [47], that the mismatch leads to a deformation of the lipid bilayer surfaces (cf. Fig. 5b above with Fig. 1 in Ref. 34), which in turn creates a lateral capillary force between two protein molecules [34].

In the experiments of Yoshimura et al. [17-20] the production of ultrathin suspension film of uniform thickness on mercury substrate was of crucial importance for obtaining of well ordered 2D array from water soluble globular proteins and protein complexes. In such thin wetting films the capillary forces are operative and bring about fast ordering of the protein molecules. As mentioned above, the energy of capillary attraction between two protein molecules is in the order of dozens of  $kT$  ( $kT$  is the thermal energy). Certainly, additional short-ranged electrostatic and hydrophobic interactions are also important for the mutual alignment of the non-spherical protein molecules with respect to each other and to the substrate. The presence of glucose in the suspension [18] seems to be important for preservation of the protein structure upon drying. Similar combination of long-ranged capillary forces and hydrodynamic fluxes, with short-ranged specific interactions (electrostatic, hydrophobic, etc.) may explain the mechanism of 2D ordering in the well established "mica spreading technique" [14-16], where a thin suspension film is formed on molecularly smooth mica substrate.

## REFERENCES

1. Denkov, N.D., Velev, O.D., Kralchevsky, P.A., Ivanov, I.B., Yoshimura, H. and Nagayama, K., *Nature (London)*, **361**, 26 (1993); *Langmuir*, **8**, 3183 (1992).
2. Kralchevsky, P.A., Paunov, V.N., Ivanov, I.B. and Nagayama, K., *J. Colloid Interface Sci.*, **151**, 79 (1992).
3. Kralchevsky, P.A., Paunov, V.N., Denkov, N.D., Ivanov, I.B. and Nagayama, K., *J. Colloid Interface Sci.*, **155**, 420 (1993).
4. Kralchevsky, P.A. and Nagayama, K., *Langmuir*, **10**, 23 (1994).
5. Alfrey Jr., T., Bradford, E.B. and Vanderhoff, J.W., *J. Opt. Soc. Am.*, **44**, 603 (1954).
6. Krieger, I.M. and O'Neill, F.M., *J. Am. Chem. Soc.*, **90**, 3114 (1968).
7. Goodwin, J.W., Ottewill, R.H. and Parentich, A., *J. Phys. Chem.*, **84**, 1580 (1980).
8. Deckman, H.W. and Dunsmuir, J.H., *Appl. Phys. Lett.*, **41**, 337 (1982).
9. Deckman, H.W., Dunsmuir, J.H., Garoff, S., McHenry, J.A. and Peiffer, D.G., *J. Vac. Sci. Technol. B*, **6**, 333 (1988).
10. Hayashi, S., Kumamoto, Y., Suzuki, T. and Hirai, T., *J. Colloid Interface Sci.*, **144**, 538 (1991).
11. Kralchevsky, P.A., Denkov, N.D., Paunov, V.N., Velev, O.D., Ivanov, I.B., Yoshimura, H. and Nagayama, K., *J. Phys.: Condens. Matter*, **6**, A395 (1994).
12. Dushkin, C.D., Nagayama, K., Miwa, T. and Kralchevsky, P.A., *Langmuir*, **9**, 3695 (1993).
13. Dushkin, C.D., Yoshimura, H., Nagayama, K., *Chem. Phys. Lett.*, **204**, 455 (1993).
14. Harris, J.R., *Micron Microscopica Acta*, **22**, 341 (1991).
15. Jap, B.K., Zulauf, M., Scheybani, T., Hefti, A., Baumeister, W., Aebi, U. and Engel, A., *Ultramicroscopy*, **46**, 45 (1992).
16. Horne, R.W., *Adv. Virus Res.*, **24**, 173 (1979).
17. Yoshimura, H., Endo, S., Matsumoto, M., Nagayama, K. and Kagawa, Y., *J. Biochem.*, **106**, 958 (1989).
18. Yoshimura, H., Matsumoto, M., Endo, S. and Nagayama, K., *Ultramicroscopy*, **32**, 265 (1990).
19. Akiba, T., Yoshimura, H. and Namba, K., *Science*, **252**, 1544 (1991).
20. Nagayama, K., *Nanobiology*, **1**, 25 (1992).
21. Henderson, R. and Unwin, P.N.T., *Nature (London)*, **257**, 28 (1975); Unwin, P.N.T. and Zampighi, G., *Nature (London)*, **283**, 545 (1980).
22. Dimitrov, A.D., Dushkin, C.D., Yoshimura, H., and Nagayama, K., *Langmuir*, **10**, 432 (1994).
23. Morita, M., Matsumoto, M., Usui, S., Abe, T., Denkov, N.D., Velev, O.D. and Ivanov, I.B., *Colloids Surfaces*, **67**, 81 (1992).

24. Lazarov, G.S., Denkov, N.D., Velev, O.D., Kralchevsky, P.A. and Nagayama, K., *J. Chem. Soc.: Faraday Trans.*, 90, 2077 (1994).
25. Denkov, N. D., Yoshimura, H., Kouyama, T. and Nagayama, K., *Phys. Rev. Lett.* (1996) in press.
26. Kouyama, T., Yamamoto, M., Kamiya, N., Iwasaki, H., Ueki, T., and Sakurai, I., *J. Mol. Biol.*, 236, 990 (1994).
27. Dubochet, J., Adrian, M., Chang, J.-J., Homo, J.-C., Lepault, J., McDowell, A.W. and Schultz, P., *Quart. Rev. Biophys.*, 21, 129 (1988).
28. Nicolson, M.M., *Proc. Cambridge Philos. Soc.*, 45, 288 (1949).
29. Chan, D.Y.C., Henry, J.D. and White, L.R., *J. Colloid Interface Sci.*, 79, 410 (1981).
30. Gifford, W.A. and Scriven, L.E., *Chem. Eng. Sci.*, 26, 287 (1971).
31. Paunov, V.N., Kralchevsky, P.A., Denkov, N.D. and Nagayama, K., *J. Colloid Interface Sci.*, 157, 100 (1993).
32. Paunov, V.N., Kralchevsky, P.A., Denkov, N.D., Ivanov, I.B. and Nagayama, K., *Colloids Surfaces*, 67, 119 (1992).
33. Kralchevsky, P.A., Paunov, V.N., Denkov, N.D. and Nagayama, K., *J. Colloid Interface Sci.*, 167, 47 (1994).
34. Kralchevsky, P.A., Paunov, V.N., Denkov, N.D. and Nagayama, K., *J. Chem. Soc.: Faraday Trans.*, 91, 3415 (1995).
35. Kralchevsky, P.A., Paunov, V.N. and Nagayama, K., *J. Fluid Mech.*, 299, 105 (1995).
36. Camoin, C., Roussel, J.F., Faure, R. and Blanc, R., *Europhys. Lett.*, 3, 449 (1987).
37. Velev, O.D., Denkov, N.D., Paunov, V.N., Kralchevsky P.A. and Nagayama, K., *Langmuir*, 9, 3702 (1993).
38. Dushkin, C.D., Kralchevsky, P.A., Yoshimura, H. and Nagayama, K., *Phys. Rev. Lett.*, 75, 3454 (1995).
39. Dushkin, C.D., Kralchevsky, P.A., Paunov, V.N., Yoshimura H. and Nagayama K. *Langmuir*, 12, 641 (1996).
40. Velev, O.D., Denkov, N.D., Paunov, V.N., Kralchevsky, P.A. and Nagayama, K., *J. Colloid Interface Sci.*, 167, 66 (1994).
41. Petkov, J.T., Denkov, N.D., Danov, K.D., Velev, O.D., Aust, R. and Durst, F., *J. Colloid Interface Sci.*, 172, 147 (1995).
42. Danov, K.D., Aust, R., Durst, F. and Lange, U., *J. Colloid Interface Sci.*, 175, 36 (1995).
43. Petkov, J.T., Danov, K.D., Denkov, N.D., Aust, R. and Durst, F., *Langmuir* (1995) submitted for publication.
44. Lewis, B.A. and Engelman, D.M., *J. Mol. Biol.*, 166, 203 (1983).
45. Chen, Y.S. and Hubbel, *Exp. Eye Res.*, 17, 517 (1973).
46. Huschilt, J.C., Hodges, R.S. and Davis, J.H., *Biochem*, 24, 1377 (1985).
47. Israelachvili, J.N., *Biochim. Biophys. Acta*, 469, 221 (1977).